PHYSICAL REVIEW B VOLUME 19, NUMBER 8 15 APRIL 1979

# Field-effect mobility in quantized accumulation layers on ZnO surfaces

M. Nitzan, Y. Grinshpan, and Y. Goldstein
*The Racah Institute of Physics, Hebrew University of Jerusalem, 91000 Israel*
(Received 12 January 1978)

Measurements are reported of the field-effect mobility $\mu_{FE}$ in strong accumulation layers on the polar surfaces of ZnO crystals. Results are presented of $\mu_{FE}$ as a function of surface electron density $\Delta N$ (in the range $10^{12}$–$10^{14}$ cm$^{-2}$) and of temperature (2–300 K). By a suitable integration procedure it has been possible to derive from the field-effect data the ordinary conductivity mobility $\mu$ as a function of $\Delta N$ and temperature. At a fixed temperature both $\mu_{FE}$ and $\mu$ initially rise with increasing $\Delta N$, reach a maximum at $\Delta N \approx (2\text{–}5)\times 10^{13}$ cm$^{-2}$, and then gradually decrease with a further increase in $\Delta N$. For high $\Delta N$ ($\gtrsim 10^{13}$ cm$^{-2}$) $\mu_{FE}$ and $\mu$ are practically temperature independent; for low $\Delta N$ ($\lesssim 3\times 10^{12}$) they decrease strongly with decreasing temperature, indicating carrier localization at low temperatures. The results of the conductivity mobility $\mu$ agree well with those of the Hall mobility $\mu_H$ reported earlier, and provide further support for the model proposed there of charged scattering centers consisting of large conglomerates of surface ions.

## I. INTRODUCTION

ZnO is of particular interest for studies of quantized surface layers because of the huge electron densities that can be obtained on its surface with relative ease.[1-7] These densities are about one order of magnitude larger than those obtainable on silicon metal-oxide-semiconductor structures. In contrast to silicon channels, however, only relatively few studies of mobility were reported on ZnO. Heiland[3] and Krusemeyer[8] measured the field-effect mobility $\mu_{FE}$ on the prism surface of ZnO "needle" crystals. Van Hove[9] studied relaxation effects in the field-effect signal. Kohl and Heiland[10] performed Hall-effect measurements on cleaved polar surfaces of ZnO at liquid-nitrogen temperature. They explored the range of relatively low surface-electron concentrations $\Delta N$ of $10^{7}-10^{13}$ cm$^{-2}$. Recently, the present authors[7] have reported on detailed measurements of the Hall-effect mobility in quantized accumulation layers on the polar surfaces of ZnO. The measurements were performed in the surface-electron concentration range of $10^{12}-10^{14}$ cm$^{-2}$, and as a function of temperature from 300 down to 2 K.

In this paper we present results on the field-effect mobility $\mu_{FE}$ obtained over the same ranges of carrier concentrations and temperatures. Most of the data pertain to the polar "oxygen" (000$\bar{1}$) face, but some results on the "zinc" (0001) face are also included. By a suitable integration procedure we were able to derive from the field-effect data the usual conductivity mobility $\mu$ as well, and this will also be presented as a function of temperature and $\Delta N$.

The present results extend and supplement our previous results[7] of Hall-effect mobility. We find that at a fixed temperature the conductivity mobility initially increases with $\Delta N$, reaches a maximum at $\Delta N \approx (2-5)\times 10^{13}$ cm$^{-2}$, and then gradually decreases with increasing $\Delta N$. As a function of temperature, the mobility at high $\Delta N$ is found to be temperature independent. At $\Delta N$ below about $10^{13}$ cm$^{-2}$, both the field-effect mobility and the conductivity are strongly temperature dependent, decreasing with decreasing temperatures. This temperature dependence is attributed to carrier localization at low temperatures. These findings are compatible with the Hall-mobility data reported earlier,[7] and support the model proposed there of charged scattering centers consisting of large conglomerations of surface ions.

## II. EXPERIMENTAL

The experimental arrangement was similar to that in Ref. 7. Samples of ZnO single crystals were supplied by the Airtron Co. The samples were cut to typical dimensions of $10\times 2\times 1$ mm$^3$, with the hexagonal $c$- axis perpendicular to the large surfaces. After lapping the polar (i.e., the large) surfaces, the samples were cleaned and etched in concentrated HCL. This etch enables one to distinguish between the (000$\bar{1}$) oxygen face and the (0001) zinc face.[1] Eight indium contacts were soldered to each sample; two of these on the end faces to serve as current contacts, while the others were distributed on both sides, along the dimension of the oxygen surface. All faces except the investigated surface were masked with Picein to prevent them from influencing the conductivity. The sample was mounted on a boron nitride substrate which provided a good thermal contact with, and electrical insulation from, the sample holder. A calibrated carbon resistor and a copper-con-

 

stantan thermocouple were connected to the substrate, just underneath the crystal, for temperature measurements. The sample was then inserted into a cryogenic system where the temperature could be varied between 1.6 and 320 K. The temperature was controlled by a heater with a temperature stabilizer, and around 4.2 K—by helium exchange gas.

The samples used were insulating (Li doped), of bulk resistivity well over $10^8$ Ω -cm. Two methods were employed to produce high surface-electron densities: illumination of the surface[2,4,5] with band-gap light (uv) while in a vacuum of about $10^{-5}$ Torr, or exposure to $He^+$ ions.[6] With the first method we could produce medium-strong accumulation layers of surface-electron densities $\Delta N$ up to about $4\times10^{13}$ $cm^{-2}$. After the illumination the accumulation layer could be maintained for long periods by simply leaving the sample in vacuum or in a helium atmosphere. Letting dry oxygen into the system destroyed the accumulation layer gradually. With the second method (electrical discharge in helium) much higher surface-electron concentrations could be obtained, up to $10^{14}-2\times10^{14}$ $cm^{-2}$. Such strong accumulation layers could generally be maintained for long times only when cooled below ~100 K. At higher temperatures these very strong accumulation layers usually decayed slowly, even at pressures of $10^{-5}$ Torr. Admitting oxygen into the system at room temperature caused a fast decrease in the accumulation layer, as in the case of illumination.

In order to measure the field-effect mobility, we used a small conducting "field plate." The field plate was pressed against the sample' s surface with a thin (~10 μm) sheet of mylar insulating the plate from the sample. The plate covered about half the sample's surface (around its middle), and the geometrical capacitance $C_g$ between the field plate and the sample was of the order of 10 pF (~100 pF/$cm^2$). When the accumulation layer was produced by illumination, the field plate consisted of a transparent conducting quartz. When the accumulation layer was prepared by exposure to $He^+$ ions, the field plate (made now of metal) had to be removed for the time of the electrical discharge. This was controlled from outside of the cryostat by means of a micromanipulator.

A floated constant-current source, consisting of a battery and a large (adjustable) resistance provided the measuring current $I$ through the ZnO sample. The voltage across a series resistance served to monitor the current. A voltage pulse $V_p$ of about 100 V was applied across the field plate and the ZnO sample. The charge $\delta Q_s$ (per $cm^2$) induced by the pulse at the ZnO surface is given by

$$\delta Q_s = -C_g V_p/wl' , \tag{1}$$

where $w$ is the width of the crystal and $l'$ is the length of the field plate. The change $\delta\sigma'$ in the surface conductance $\Delta\sigma$ (per square) of that part of the sample underneath the field plate is given by

$$\delta\sigma' = -(l'/w)\delta R'/R'^2 . \tag{2}$$

Here $\delta R'$ is the change in $R'$, the resistance of the part of the sample underneath the field plate. The field-effect mobility $\mu_{FE}$ is defined (for the case of electron accumulation layers considered) as[11]

$$\mu_{FE} = -\delta\sigma'/\delta Q_s = -(l^2/C_g V_p)\delta R'/R'^2 . \tag{3}$$

Now, if $l$ is the distance between two voltage probes ($l>l'$) and $R$ is the sample's resistance between those probes, then for a homogeneous sample $l^2/R^2 = l'^2/R'^2$ and, of course, $\delta R = \delta R'$. Thus we can rewrite Eq. (3)

$$\mu_{FE} = -(l^2/C_g V_p)\delta R/R^2 , \tag{4}$$

where now $R$ is the resistance between the probes. The change $\delta R$ was measured by the change $\delta V$ in the voltage $V$ across the probes; $\delta R = \delta V/I$. In order to measure the geometrical capacitance $C_g$, we applied a voltage pulse (amplitude $V_c$) across $C_g$ and a known capacitor $C(>>C_g)$ in series with $C_g$. The voltage $V_c'$ across $C$ reaches eventually the value

$$V_c' \approx V_c(C_g + C_p)/C , \tag{5}$$

where $C_p$ is the parasitic capacitance between the field plate and the leads to the sample. Whereas $C_p$ charges up practically immediately, $C_g$ is connected in series with the sample's resistance and takes some time to charge up. Thus the signal $V'$ displays a fast rise followed by a much slower rise. The two components are easily resolvable, and enable the determination of $C_g$, the capacitance of interest, without the interfering effect of the parasitic capacitance.

The voltage pulses used for measuring $\mu_{FE}$ were flat pulses of about 100 V in amplitude, of 1 μsec rise and fall times and of 10 msec duration. The change in the surface-electron density due to such a pulse was typically about $5\times10^{10}$ $cm^{-2}$. The signal $\delta V$ measured on the oscilloscope varied from a few tenths of a millivolt to a few tens of millivolts, depending on the resistance of the sample (surface). In all cases the shape of the field-effect signal was square, identical with that of the applied pulse; no relaxation effects such as those that might arise from the presence of surface states were detected. We checked for possible large time-constant relaxations, up to 10 min, but did not find any. Thus if any surface states were active in the regime investigated by us (strong

accumulation layers), their capture and release times have to be less than a microsecond or so or larger than minutes.

The procedure used in measuring $\mu_{FE}$ as a function of temperature and of $\Delta N$ was as follows. While at room temperature, the sample was illuminated or exposed to $He^+$ ions (depending on the range of $\Delta N$ desired) until the surface resistance reached (with either method) its lowest value, corresponding to the strongest accumulation layer. Next, $\mu_{FE}$ was measured as a function of the temperature by cooling the sample down to liquid-nitrogen or liquid-helium temperatures. The sample was then heated up to room temperature and its resistance checked against its value before the cool-down cycle. The absence of any change in resistance ensured that the sample did not adsorb any oxygen, and thus that the surface conditions did not change during the measurement cycle. In most cases the resistance values matched to within 1%–2%. In order to change $\Delta N$, oxygen was admitted into the cryostat (again at room temperature) and left inside until the sample resistance reached a desired value. At this point the cryostat was again evacuated or filled up with helium, and another set of data of $\mu_{FE}$ vs $T$ (for a lower value of $\Delta N$) was taken.

The usual conductivity mobility $\mu$ is defined as $\mu\sigma/e\Delta N$ (where $e$ is the magnitude of the electronic charge), and is in general different from $\mu_{FE}$. From the data described above one can readily construct, at each temperature, a plot of $\mu_{FE}$ as a function of the surface conductivity $\Delta\sigma$. The change $\Delta N_{12}$ in surface-electron density between condition 1 (surface conductivity $\Delta\sigma_1$) and condition 2 ($\Delta\sigma_2$) of the surface can then be obtained by integration,

$$\Delta N_{12} = -\Delta Q_{s12}/e = -(1/e)\int_{\Delta\sigma_1}^{\Delta\sigma_2} \frac{dQ_s}{d\sigma} d\sigma$$

$$\approx (1/e)\int_{\Delta\sigma_1}^{\Delta\sigma_2} (1/\mu_{FE}) d\sigma. \qquad (6)$$

It should be noted that the integration yields the change $\Delta Q_{s12}$ in the total induced charge, mobile and immobile. Only when this entire charge is mobile does $\Delta Q_{s12}/e$ represent the change $\Delta N_{12}$ in the density $\Delta N$ of *free* electrons as defined in the conventional manner.[11] This point will be discussed below.

As has already been mentioned above, medium-strong accumulation layers were obtained by uv illumination. The measurements in this region could be extended to very low values of $\Delta N$ and extrapolated to $\Delta\sigma = 0$. Thus it was possible to evaluate the integral in Eq. (6) starting from $\Delta\sigma_1 = 0$, and hence to obtain the absolute value of $\Delta N$. Measurements performed on the very strong accumulation layers (using $He^+$ ions), on the other hand, could not be extended to low $\Delta N$ because of homogeneity problems. In these cases only the differences $\Delta N_{12}$ could be derived from the data, starting the integration from the lowest $\Delta\sigma_1$ attained. The absolute magnitudes of the $\Delta N$ values for different surface conditions were then obtained by adjusting the highest $\Delta N$ value to that determined by simultaneous Hall-effect measurements.[7] Once the $\Delta N$ vs $\Delta\sigma$ plot at each temperature has been determined, the conductivity mobility $\mu$ as a function of $\Delta N$ is given, by definition, by $\mu = \Delta\sigma/e\Delta N$.

## III. RESULTS

The measurements were performed on a variety of samples and were repeated on some samples a few times after renewed surface preparation. The results on the same sample were found to be fairly reproducible, while they varied somewhat from sample to sample. The main features, however, were common to all measurements: the field-effect mobility increases sharply with increasing surface-electron concentration at low values of $\Delta N$, reaches a maximum, and then at large $\Delta N$ decreases gradually with a further increase in $\Delta N$. Typical results obtained at room temperature are shown in Fig. 1. Here the field-effect mobility $\mu_{FE}$ is plotted as a function of the surface conductivity $\Delta\sigma/e$ (in units of the electronic charge). The mobility is seen to rise at first sharply from

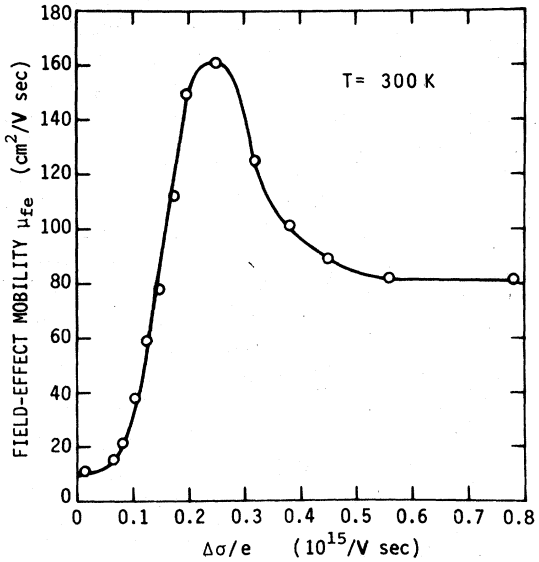


FIG. 1. Typical results of field-effect mobility $\mu_{FE}$ as a function of surface conductivity (in units of the electronic charge $e$) at room temperature.

almost zero at $\Delta\sigma = 0$ to the peak value (about 160 $cm^2/V$ sec) at $\Delta\sigma/e = 2.5 \times 10^{14}$ $(V\,sec)^{-1}$. At larger $\Delta\sigma$, the mobility decreases, first rapidly and then more gradually. This gradual decrease continues up to the strongest accumulation layers we succeeded into producing ($\Delta\sigma$ values much higher than those shown in Fig. 1). The conductivity mobility $\mu$ which corresponds to $\mu_{FE}$ in Fig. 1 varies much less rapidly. Initially, it rises from about 10 to about 80 $cm^2/V$ sec, and then gradually decreases (see below). There is no prominent peak, as contrasted to the peak apparent in the plot of $\mu_{FE}$ vs $\Delta\sigma$. The latter originates from the nature of $\mu_{FE}$ as a differential quantity. One can express $\mu_{FE}$ as

$$\mu_{FE} = \frac{-d\sigma}{dQ_s} = \frac{d(\mu Q_s)}{dQ_s} = \mu + Q_s \frac{d\mu}{dQ_s}. \tag{7}$$

Thus, because of the last term in Eq. (7), any variation of $\mu$ with $Q_s$ is multiplied by $Q_s$ and is thus amplified in the $\mu_{FE}$ vs $Q_s$ curve.

Figures 2–10 show typical results of the measurements on several ZnO samples. Extensive Hall-effect measurements on these samples were presented in Ref. 7, and for identification purposes the samples are labeled identically as in Ref. 7. The accumulation layers were prepared by one of the two methods described above. Most of the results shown pertain to the oxygen face, but some are for the zinc face. In Fig. 2 the field-effect mobility $\mu_{FE}$ is plotted as a function of temperature for different values of the surface electron-density $\Delta N$, as marked. The accumulation layer was produced by exposure to $He^+$ ions and the $\Delta N$ values correspond to the high-density range of $(1.9-11) \times 10^{13}$ $cm^{-2}$. As has already been mentioned above and will be discussed later, the absolute values of $\Delta N$ in this regime were derived from Hall-effect data. For most of the $\Delta N$ values shown, $\mu_{FE}$ is seen to increase with decreasing temperatures all the way down to 4.2 K. Only for the two lowest concentrations, $\Delta N = 1.9$ and $2.2 \times 10^{13}$ $cm^{-2}$, does $\mu_{FE}$ decrease a little at the lowest temperatures.

Figure 3 shows the field-effect mobility as a function of temperature in the lower $\Delta N$ range. Here the accumulation layer was produced by uv illumination and the results were taken on a different sample than that of Fig. 2. The different curves correspond again to different $\Delta N$ values, as marked. These $\Delta N$ values are typical for

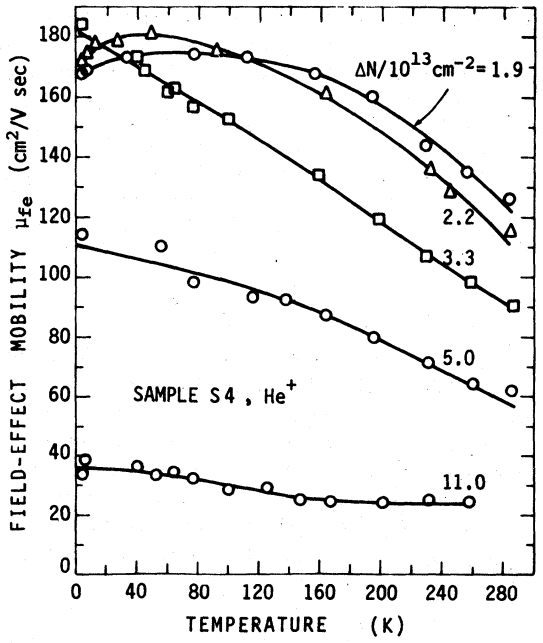


FIG. 2. Field-effect mobility $\mu_{FE}$ as a function of temperature for different surface-electron concentrations $\Delta N$, as marked. The measurements were performed on the oxygen face and the accumulation layers were produced by exposure to $He^+$ ions.

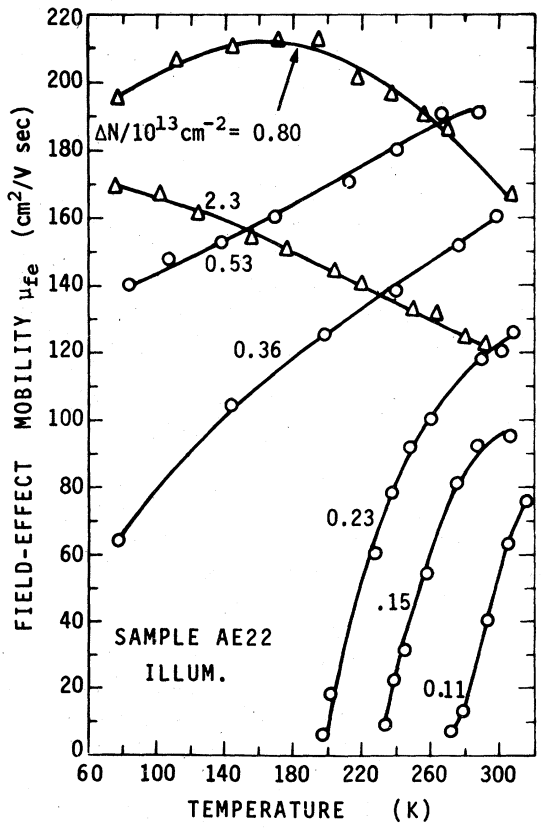


FIG. 3. Field-effect mobility $\mu_{FE}$ as a function of temperature for different surface-electron concentrations $\Delta N$, as marked. The measurements were performed on the oxygen face and the accumulation layers were produced by uv illumination.

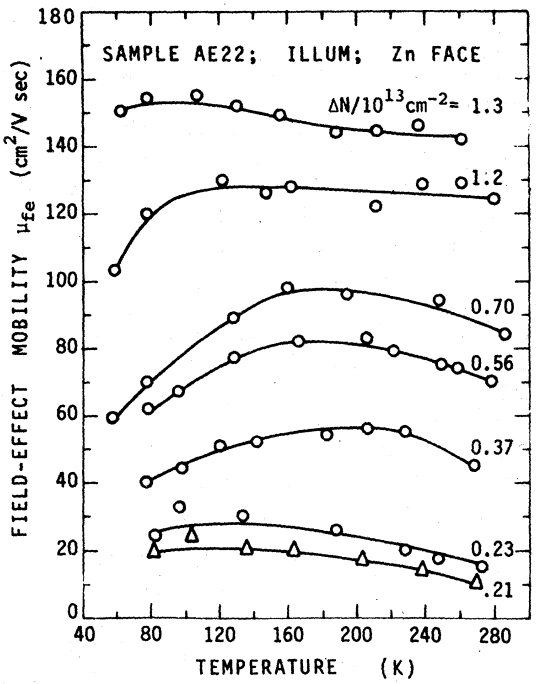


FIG. 4. Field-effect mobility $\mu_{FE}$ as a function of temperature for different surface-electron concentrations $\Delta N$, as marked. The measurements were performed on the zinc face and the accumulation layers were produced by uv illumination.

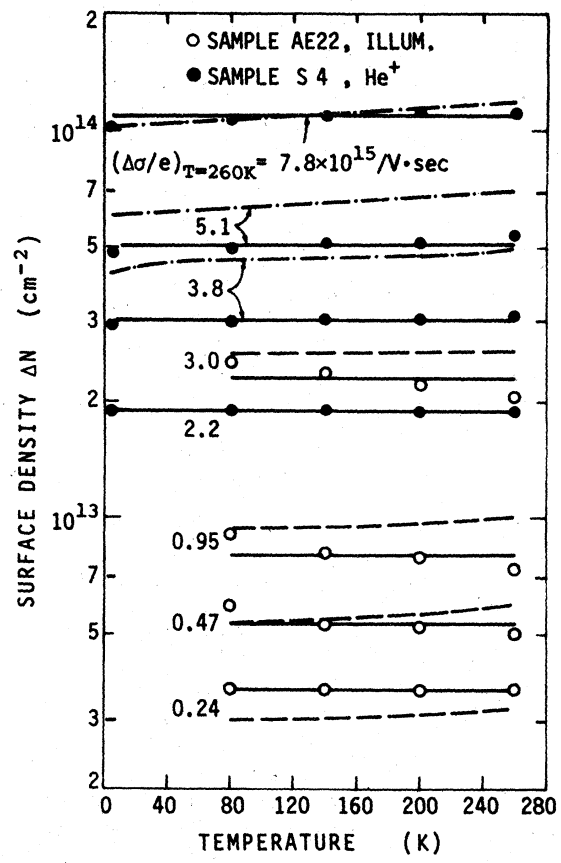


FIG. 5. Surface-electron concentration $\Delta N$ on the oxygen face as a function of temperature for different surface conditions. The different surface conditions are characterized by the values of the surface conductivity $\Delta\sigma/e$ at 260 K, as marked. The data are for two different samples, the accumulation layers on one having been produced by uv illumination (open circles) and on the other by exposure to $He^+$ ions (full circles). Results obtained by Hall-effect measurements carried out simultaneously are also included (dashed and dashed-dotted curves) for comparison purposes.

accumulation layers obtainable by illumination. In contrast to the case of the high-$\Delta N$ range, the values of $\Delta N$ in Fig. 3 were obtained by integrating Eq. (6) from $\Delta\sigma = 0$, as explained above. Inspection of Fig. 3 reveals that the behavior of $\mu_{FE}$ in this relatively low-$\Delta N$ range is quite different from that displayed by Fig. 2. Here $\mu_{FE}$ decreases sharply with decreasing temperatures at very low $\Delta N$, more moderately at higher $\Delta N$ values, and only at the highest $\Delta N$ values shown, which overlap the low-$\Delta N$ range in Fig. 2, does $\mu_{FE}$ increase with decreasing temperature. The data in Figs. 2 and 3 for this overlap range are very similar. It appears that the maximum in the $\mu_{FE}$ vs $T$ curve shifts to higher temperatures the lower $\Delta N$ is. The most pronounced feature in the data of Fig. 3 is undoubtedly the very rapid decrease of $\mu_{FE}$ with decreasing temperatures at low $\Delta N$ values. This points to carrier localization at low T and/or low $\Delta N$, as will be discussed below.

Similar results, obtained for the same sample as in Fig. 3, but on the zinc surface, are shown in Fig. 4. For this face, only the low-$\Delta N$ range, as produced by uv illumination, could be investigated. The highest electron concentration attained was $1.3 \times 10^{13}$ cm$^{-2}$, less than half that reached on the oxygen surface by illumination. Comparing the results to those Fig. 3, we see that the values of the field-effect mobility on the zinc surface are usually lower than those on the oxygen surface. On the other hand, there is no strong temperature dependence of the mobility on the zinc surface, even for surface densities as low as $2 \times 10^{12}$ cm$^{-2}$. A similar behavior has been observed for the prism surfaces. It appears then that on both faces, if carrier localization is at all present, it must be much weaker.

So far we have presented runs in which $\mu_{FE}$ and $\Delta\sigma$ were simultaneously measured as functions of temperature, for different (fixed) surface conditions, i.e., for different accumulation layers. From these measurements one can readily con-

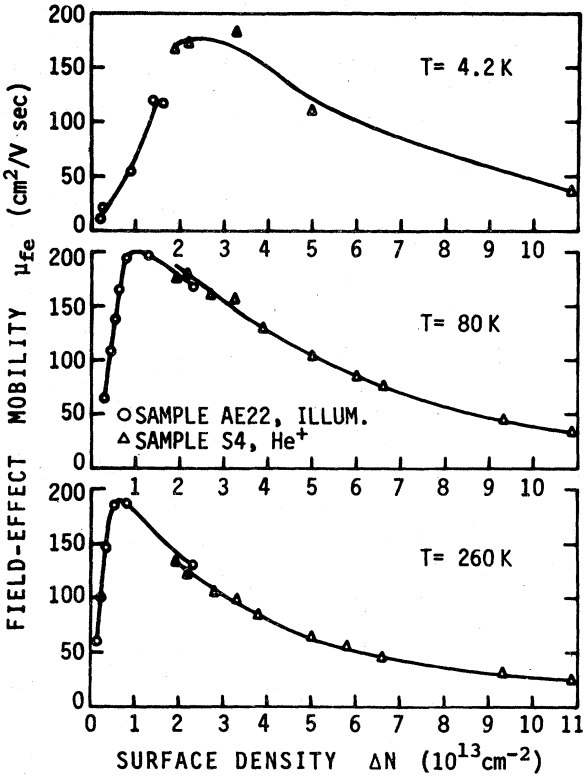


FIG. 6. Field-effect mobility $\mu_{FE}$ as a function of surface-electron concentration $\Delta N$ at three different temperatures, as marked. The measurements were performed on the oxygen faces of two different samples for the two different ranges of $\Delta N$. The accumulation layers in the low- and high-$\Delta N$ ranges have been produced by uv illumination and by exposure to $He^+$ ions, respectively.

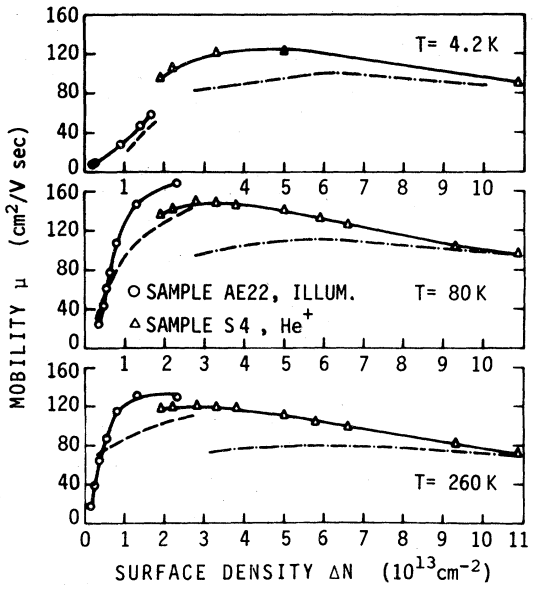


FIG. 7. Conductivity mobility $\mu$ as a function of the surface-electron concentration at three different temperatures, as marked. These curves were derived from the data in Fig. 6 by the integration procedure described in the text. The corresponding curves for the Hall mobility (dashed and dash-dotted curves) measured simultaneously are also shown for comparison purposes.

struct plots of $\mu_{FE}$ against $\Delta\sigma$ for different temperatures, such as the plot for $T = 300$ K shown in Fig. 1. The difference $\Delta N_{12}$ in the surface density $\Delta N$ between any two surface conditions (characterized by $\Delta\sigma_1$ and $\Delta\sigma_2$) can then be obtained by integration, as explained above [see Eq. (6)]. The temperature dependence of $\Delta N$ obtained by this procedure for two samples is shown in Fig. 5. The four curves passing through the open circles correspond to a sample on which accumulation has been produced by uv illumination. Here the integration could be started from $\Delta\sigma_1 = 0$, so that $\Delta N_{12}$ yields $\Delta N$ directly. The other curves (full circles) were obtained for a different sample in which accumulation has been produced by exposure to $He^+$. In this case $\Delta\sigma_1 = 0$ could not be obtained, and the constant of integration separating $\Delta N$ and $\Delta N_{12}$ was determined from a single value of $\Delta N$ ($10^{14}$ cm$^{-2}$) as obtained from Hall-effect measurements carried out on the same sample. The different curves in Fig. 5 are for different surface conditions, as characterized by the measured values of the surface conductivity $\Delta\sigma/e$ at 260 K. It is seen that $\Delta N$ is essentially independent of temperature over the entire ranges of $\Delta N$ and $T$ shown. Also shown in Fig. 5 (dashed and dashed-dotted curves) are the values of $\Delta N$ obtained from Hall-effect measurements. These values agree within about 30% to the field-effect results and are usually higher.

It should be pointed out that the values of $\Delta N$ obtained by integrating Eq. (6) include all the induced excess surface electrons, whether mobile or immobile. This is because $\delta Q_s$, appearing in the definition of $\mu_{FE}$ [Eq. (3)], includes *all* the induced charge (mobile and immobile). As has already been pointed out in Sec. II, we did not detect relaxation effects associated with surface states. This is only to be expected because for $\Delta N \gtrsim 10^{12}$ cm$^{-2}$ the conduction-band edge at the surface lies below the Fermi level,[12,13] and any surface states present in the forbidden band gap should all be filled. Thus at the high electron densities dealt with here no surface states, in the ordinary sense, are expected to be active.

After determining the value of $\Delta N$ for the different surface conditions, one can plot $\mu_{FE}$ as a

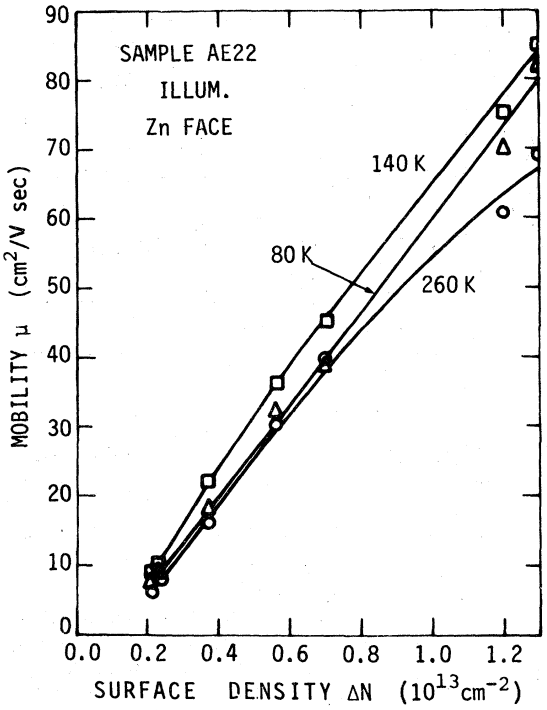


FIG. 8. Conductivity mobility $\mu$ as a function of surface-electron concentration $\Delta N$ at three different temperatures, as marked. The measurements were performed on the zinc face and the accumulation layers were produced by uv illumination.

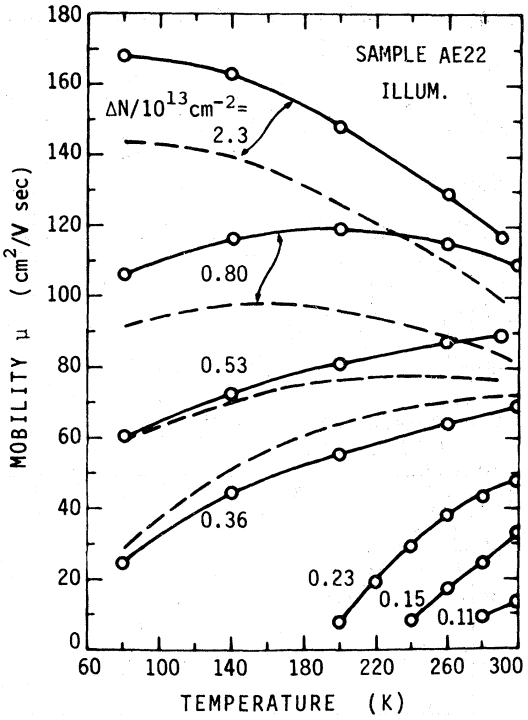


FIG. 10. Conductivity mobility $\mu$ as a function of temperature for different surface concentrations $\Delta N$, as marked. The accumulation layers were produced by uv illumination. Hall-effect data are also included for comparison.

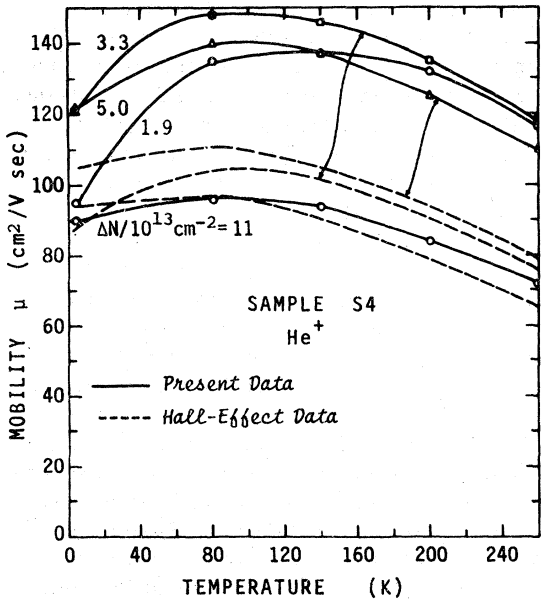


FIG. 9. Conductivity mobility $\mu$ as a function of temperature for different surface concentrations $\Delta N$, as marked. The accumulation layers were produced by exposure to $He^+$ ions. Hall-effect data are also included for comparison.

function of $\Delta N$. Such plots are shown in Fig. 6 for three different temperatures. The common feature of the curves is the sharp rise of $\mu_{FE}$ with $\Delta N$ at low $\Delta N$ and the gradual decrease at large $\Delta N$. The position of the maximum of $\mu_{FE}$ is temperature dependent and moves to lower $\Delta N$ as the temperature increases. The data for each temperature in Fig. 6 were obtained on two samples, one to cover the low-$\Delta N$ range (accumulation produced by illumination) and the other to attain the high-$\Delta N$ range ($He^+$ exposure). The agreement in the overlap region is seen to be quite good.

The behavior of $\mu_{FE}$ on the zinc and prism faces was similar to that on the oxygen face in the sense that it too increases with increasing $\Delta N$ at low $\Delta N$. However, we were unable to produce very strong accumulation layers on these faces, and the measurements were performed only in the $\Delta N$ range of up to about $10^{13}$ $cm^{-2}$.

In Fig. 7 we plot the conductivity mobility $\mu$ as obtained by the integration procedure described above against $\Delta N$ for the same two samples and the same three temperatures as in Fig. 6. As in the data of $\mu_{FE}$, the conductivity mobility is seen

to rise quite rapidly at low $\Delta N$ and then to decrease gradually. Here, as well, the maximum shifts to lower $\Delta N$ at higher temperatures. Thus $\mu$ behaves similarly to $\mu_{FE}$, but its variation with $\mu$ is more gradual. For comparison purposes, we have included in Fig. 7 Hall mobility measurements carried out on the same samples (dashed and dashed-dotted curves). The Hall mobility behaves similarly to $\mu$, but its values are somewhat lower. At the highest electron concentrations, the two mobilities are, of course, identical. This is the result of the procedure used in determining $\Delta N$ for the high-concentration range (see above).

The dependence of the conductivity mobility $\mu$ on $\Delta N$ on the zinc surface is shown in Fig. 8 for three temperatures. Only the low-$\Delta N$ range was attainable, and in this range the behavior is very similar to that of the oxygen surface (Fig. 7). Notice that the horizontal scale in Fig. 8 has been expanded, and the entire $\Delta N$ range shown here corresponds to about one tenth of the $\Delta N$ range shown in Fig. 7.

Figures 9 and 10 show the variation of the conductivity mobility $\mu$ with temperature. Figure 9 covers the high-$\Delta N$ range, while Fig. 10 covers the low-$\Delta N$ range. One can immediately see that at high $\Delta N$ the mobility depends only weakly on $T$ (Fig. 9). In this range, the mobility at first increases somewhat with decreasing temperature and only at the lowest temperatures does it decrease a little. At lower $\Delta N$ values (Fig. 10), the mobility maximum obtains at higher temperatures, and eventually the mobility decreases with decreasing $T$ over the entire temperature range shown. At the lowest $\Delta N$ values shown a "freezing" of the mobility is observed as the temperature drops. Once again we see that the behavior of $\mu$ is similar to that of $\mu_{FE}$, except that its variation with $T$ is more gradual. Results of Hall-effect measurements are also included in Figs. 9 and 10 (dashed curves). The Hall mobility is again seen to behave similarly to the conductivity mobility, but corresponding pairs of curves differ somewhat.

## IV. DISCUSSION

We have presented measurements of the field-effect mobility $\mu_{FE}$ in accumulation layers on the polar faces of ZnO. The results cover wide ranges of surface-electron densities $\Delta N$ and temperatures. Although the mobility was found to vary somewhat from sample to sample, the qualitative behavior is quite general. At fixed temperatures, $\mu_{FE}$ rises rather sharply with $\Delta N$ for low $\Delta N$ and, in the case of the oxygen face, it reaches a maximum value, after which it decreases slowly with a further increase in $\Delta N$. The position of the maximum shifts towards higher $\Delta N$ values with decreasing temperature. For the zinc face the accumulation layers that could be produced were much weaker, and in this range, only the rising part of the $\mu_{FE}$ vs $\Delta N$ curve could be observed. On the oxygen face, the temperature dependence of $\mu_{FE}$ differs greatly in different ranges of $\Delta N$. For high $\Delta N$, $\mu_{FE}$ is practically independent of $T$. For $\Delta N$ around $(2-3)\times 10^{13}$ cm$^{-2}$, $\mu_{FE}$ increases with decreasing $T$ down to about 80 K and then starts to decrease. At lower $\Delta N$ values, $\mu_{FE}$ starts decreasing with decreasing $T$ already at high temperatures. For electron densities below about $3\times 10^{12}$ cm$^{-2}$ $\mu_{FE}$ decreases rapidly with decreasing temperature and appears to "freeze out". No such freeze-out of the mobility was found to occur on the zinc face down to the lowest $\Delta N$ and temperature studied.

For the moderately strong accumulation layers produced by uv illumination, it has been possible to derive from the field-effect mobility data the value of $\Delta N$ corresponding to each measured value of the surface conductivity $\Delta\sigma$. This procedure immediately yields the conductivity mobility $\mu(\equiv\Delta\sigma/e\Delta N)$ as a function of $\Delta N$ and temperature. The results so obtained are in fairly good agreement with the Hall mobility measurements carried out simultaneously on the same samples and reported previously.[7] In fact, the field-effect data are more reliable than the Hall-effect data in this range of relatively low $\Delta N$, because the latter are much more sensitive to surface nonhomogeneity frequently encountered in this $\Delta N$ range. It should be noted that trapping, in the ordinary sense, by surface or bulk states cannot contribute to the measured value of the field-effect mobility. As for surface states, in the range $\Delta N \gtrsim 10^{12}$ cm$^{-2}$ the conduction-band edge at the surface lies below the Fermi level[12,13] and any surface states that may be present in the forbidden gap should be filled up and thus inactive. Bulk states in the surface space charge channel are also unimportant because of the narrow width of the channel.[12,13] And, indeed, no relaxation effects were detected in the field effect. Thus the present results provide strong independent support for the Hall-effect data, and hence for the conclusions reached in Ref. 7. The most significant conclusion was that the dominant surface scattering at low $\Delta N$ involves charged scattering centers consisting of large conglomerates of surface ions. Further evidence for this was provided by magnetoresistance measurements[14,15] which revealed the presence on the ZnO surface of giant magnetic moments, as might arise from large ionic conglomerates. Such conglomerates were also encountered on the Si-$SiO_2$ interface.[16,17] On the oxygen face,

the ionic conglomerates give rise to carrier localization at low temperatures in the low-$\Delta N$ range. For higher $\Delta N$ the scattering centers are largely screened out and the scattering becomes dominated by surface roughness and phonons.[7] The absence of any significant carrier localization on the zinc surface is not understood.

Several scattering theories based on charged centers were worked out and were found to be reasonably successful in accounting for results of surface transport in silicon channels. These theories were reviewed briefly in Ref. 7, mostly in an attempt to account, at least qualitatively, for our data on ZnO channels. We would like to add here that another model that involves carrier-density fluctuations, not mentioned in Ref. 7, was worked out by Brews.[18] It appears that this model may be applied equally well to our data.

For the strong accumulation layers produced by exposure to $He^+$, $\Delta N$ could be determined only to within an integration constant. This is, however, only a minor limitation and does not invalidate the conclusion that $\Delta N$ is practically temperature independent (see Fig. 5) over the entire range studied (2–300 K).

Although corresponding values of the Hall mobility and the conductivity mobility differ by less than 30%, the former are consistently lower than the latter. This may indicate that the Hall factor $r_H$ is smaller than unity. Sakaki and Sugano[19] showed that at the silicon inversion channel one might expect under certain conditions that $r_H < 1$. This, however, is due to the unisotropy of the effective mass in the silicon conduction band. In ZnO, on the other hand, band-structure calculations,[20] as well as recent results on strong accumulation layers[12,13] indicate an isotropic effective mass, for which case the theory of Sakaki and Sugano predicts that $r_H \geq 1$. At the same time, Friedman[21] showed that the Hall mobility for low-mobility disordered systems may be smaller than the conductivity mobility. Our mobilities are, however, somewhat large compared to those assumed in Friedman's calculations, so that his model may not be applicable in our system.

ACKNOWLEDGMENTS

We wish to thank A. Many for many helpful suggestions and critical discussions. This work was supported in part by the National Council for Research and Development, Israel and the Kernforschungszentrum Karlsruhe GmbH, Germany.

[1]G. Heiland and P. Kunstmann, Surf. Sci. 13, 72 (1969).
[2]G. Heiland, E. Mollwo, and F. Stöckmann, Solid State Phys. 8, 193 (1958).
[3]G. Heiland, J. Phys. Chem. Solids 6, 155 (1958).
[4]A. Many, CRC, Critical Rev. Solid State Sci. 4, 515 (1974).
[5]D. Eger, Y. Goldstein, and A. Many, RCA Review 36, 508 (1975).
[6]Y. Goldstein, A. Many, D. Eger, Y. Grinshpan, G. Yaron, and M. Nitzan, Phys. Lett. 62A, 57 (1977).
[7]Y. Grinshpan, M. Nitzan, and Y. Goldstein, Phys. Rev. B 19, 1098 (1979).
[8]H. J. Krusemeyer, Phys. Rev. 114, 655 (1959).
[9]H. J. van Hove, Surf. Sci. 22, 76 (1970).
[10]D. Kohl and G. Heiland, Surf. Sci. 63, 96 (1977).
[11]A. Many, Y. Goldstein, and N. B. Grover, *Semiconductor Surfaces* (North-Holland, Amsterdam, 1965).
[12]D. Eger, A. Many, and Y. Goldstein, Surf. Sci. 58, 18 (1976).
[13]D. Eger and Y. Goldstein, Phys. Rev. B 19, 1089 (1979).
[14]Y. Goldstein and Y. Grinshpan, Phys. Rev. Lett. 39, 953 (1977).
[15]Y. Goldstein, Y. Grinshpan, and A. Many, Phys. Rev. B 19, 2256 (1979).
[16]T. H. DiStefano, Appl. Phys. Lett. 19, 280 (1971).
[17]R. Williams and M. H. Woods, J. Appl. Phys. 43, 4142 (1972).
[18]J. R. Brews, J. Appl. Phys. 46, 2181, 2193 (1975).
[19]H. Sakaki and T. Sugano, Jap. J. of Appl. Phys. 10, 1016 (1971).
[20]W. Roessler, Phys. Rev. 184, 733 (1969).
[21]L. Riedman, J. Non-Cryst. Solids 6, 329 (1971).